Brief Report

Thermal Confinement Effects in Laser-Polished AM 316L Slots: The Role of Geometry in Internal Surface Response

Aswin Karakadakattil *

Posted Date: 17 April 2026

doi: 10.20944/preprints202603.0074.v2

Keywords: laser polishing; additive manufacturing (AM) 316L; thermal confinement; depth-dependent microhardness; slot and channel geometries; microstructure–property relationship; biomedical and aerospace components

 doi:10.20944/preprints202603.0074.v2

Brief Report

Thermal Confinement Effects in Laser-Polished AM 316L Slots: The Role of Geometry in Internal Surface Response

Aswin Karkadakattil

Independent Researcher, Kasaragod 671314, India; ashwinharik20000@gmail.com

Abstract

Laser polishing (LP) is widely employed to enhance the surface quality of additively manufactured (AM) metals; however, its behaviour within deep or confined internal geometries remains insufficiently understood. Many high-performance AM components, such as biomedical implants, turbine cooling channels, and metal microfluidic systems, incorporate narrow internal features where heat-transfer conditions differ significantly from open surfaces. In this study, laser powder bed fusion (LPBF)-fabricated 316L stainless steel specimens containing ~10 mm deep slots with widths ranging from 1 to 5 mm were subjected to laser polishing using a continuous-wave fibre laser (power: 80–120 W, scan speed: 450–750 mm/s, spot size: ~80–100 μm, ~60–70% track overlap, single-pass strategy). The influence of internal geometric confinement on microstructural evolution and mechanical response was systematically investigated. A pronounced depth-dependent microhardness gradient was observed along the slot wall, with hardness decreasing from approximately 270 HV in the lower region to ~210 HV near the slot opening, with more significant gradients in narrower geometries. Quantitative grain-size analysis revealed finer grains (~8–12 μm) in the lower region and coarser grains (~18–25 μm) toward the upper region, indicating progressive grain coarsening with increasing height. These variations are attributed to geometry-dependent thermal boundary conditions, where enhanced conductive coupling to the bulk substrate in the lower region promotes higher cooling rates, while reduced thermal extraction near the slot opening results in slower solidification. The results provide clear experimental evidence that internal geometric confinement can significantly influence microstructure–property evolution during laser polishing, even under constant processing parameters. This study highlights the importance of incorporating geometric effects into post-processing strategies for AM components and offers practical insights for achieving more predictable and uniform mechanical performance in confined internal features.

Keywords: laser polishing; additive manufacturing (AM) 316L; thermal confinement; depth-dependent microhardness; slot and channel geometries; microstructure–property relationship; biomedical and aerospace components

1. Introduction

1.1. Background and Motivation

Metal additive manufacturing (AM), particularly laser powder bed fusion (LPBF) of 316L stainless steel, has enabled the fabrication of components with highly complex geometries, including internal channels, enclosed cavities, and architected features that are difficult or impossible to produce using conventional subtractive methods [1–3]. These capabilities have driven widespread adoption in high-performance applications such as biomedical implants, aerospace cooling passages, compact heat exchangers, and metal-based microfluidic systems [4–7]. Despite these advantages, LPBF-fabricated components typically exhibit surface-related limitations, including partially fused powder particles, elevated surface roughness, and microstructural heterogeneity, which can

 doi:10.20944/preprints202603.0074.v2

negatively affect fatigue performance, corrosion resistance, fluid flow behaviour, and structural reliability [8–10]. Laser polishing (LP) has emerged as a promising non-contact post-processing technique for improving surface quality. By inducing localized surface remelting, LP enables material redistribution driven by surface tension and capillary flow, reducing surface asperities and modifying near-surface microstructure [11–15]. Compared to conventional mechanical polishing, LP offers advantages for complex geometries, particularly internal or inaccessible surfaces. For open and planar surfaces, thermal behaviour during laser polishing is relatively well understood, with heat dissipation governed by conduction and convection, leading to predictable melt-pool dynamics and cooling rates [16,17]. However, in confined geometries such as deep slots or narrow internal channels, these assumptions no longer hold. Geometric confinement alters heat-flow pathways by restricting lateral conduction, reducing convective heat loss, and modifying melt-pool stability. Recent theoretical and numerical studies have demonstrated that geometric confinement and boundary conditions significantly influence melt-pool behaviour and solidification kinetics during laser processing [18–22]. Reduced heat dissipation in confined regions leads to variations in cooling rate, which directly influence grain growth and mechanical properties [23,24]. While microhardness gradients have been reported within melt pools and deposited layers in AM processes [25,26], comparatively little attention has been given to depth-dependent microstructural evolution within laser-polished confined geometries. Quantitative characterization techniques such as ImageJ-based grain analysis [27] and ASTM E112 grain-size evaluation [28] provide robust tools for such investigations; however, their application to internal geometries remains limited.

1.2. Comparison with Existing Studies

Existing studies on laser polishing have primarily focused on open or externally accessible surfaces, where thermal boundary conditions are relatively uniform and well understood [11–15]. Some investigations have explored laser polishing of internal channels; however, these studies are often limited to surface roughness evaluation and do not provide detailed insight into depth-dependent microstructural evolution [2,3]. n parallel, numerical and theoretical studies have examined melt-pool dynamics and thermal behaviour in laser-based processes, demonstrating that geometric confinement significantly influences temperature distribution, cooling rates, and solidification behaviour [18–22]. Advanced simulation and experimental studies further support these findings by highlighting the role of melt-pool instability [23-27], defect evolution, and thermal gradients in determining final microstructure [28–32]. Despite these advances, many of these studies lack direct experimental validation within confined internal geometries. Furthermore, while prior research has established relationships between cooling rate, grain size, and mechanical properties, systematic experimental quantification within laser-polished internal features remains limited [33–35].

1.3. Gap in Knowledge

Most laser polishing studies implicitly assume open-surface conditions, where heat dissipation into the bulk material and surrounding environment is relatively unconstrained [11–15]. While this assumption is valid for external surfaces, it does not accurately represent the thermal boundary conditions present in confined internal geometries. In deep or narrow slots, heat extraction pathways vary significantly along the feature depth due to differences in conductive coupling with the surrounding bulk material and exposure to the environment. Although theoretical and numerical investigations suggest that geometric confinement can modify melt-pool dynamics, thermal gradients, and cooling behaviour [29–33], additional fundamental studies on laser–material interaction, melt-pool physics, and additive manufacturing defects further support these effects [36–40]. However, systematic experimental studies quantifying depth-dependent microhardness and grain-size evolution in such geometries remain scarce. This knowledge gap is particularly important because internal surfaces often govern the long-term performance of engineering components,

 doi:10.20944/preprints202603.0074.v2

including aerospace cooling channels, biomedical implants, and microfluidic systems, where local microstructural stability and mechanical integrity are critical [41–45].

1.4. Objective of This Study

The objective of this study is to investigate the influence of confined slot geometry on microhardness and microstructural evolution during laser polishing of LPBF-fabricated 316L stainless steel. By analysing lower, middle, and upper regions of approximately 10 mm deep slots with widths ranging from 1 to 5 mm, the study quantifies depth-dependent variations in hardness and grain size under controlled processing conditions. The work aims to experimentally establish the relationship between geometric boundary conditions, cooling-rate variation, grain refinement, and mechanical response within confined internal feature.

1.5. Contribution and Novelty

This study makes the following key contributions:

- It provides systematic experimental quantification of depth-dependent microhardness variation within laser-polished internal AM slots.
- It demonstrates that geometric confinement influences hardness gradients even when nominal laser processing parameters are held constant.
- It establishes a quantitative correlation between grain-size evolution and mechanical response using ImageJ-based analysis and ASTM E112 grain-size evaluation.
- It bridges the gap between theoretical predictions of confinement-induced thermal effects and experimental observations in real AM geometries.
- It offers practical insights for optimizing laser polishing strategies in components containing confined internal features, enabling improved control over local mechanical performance.

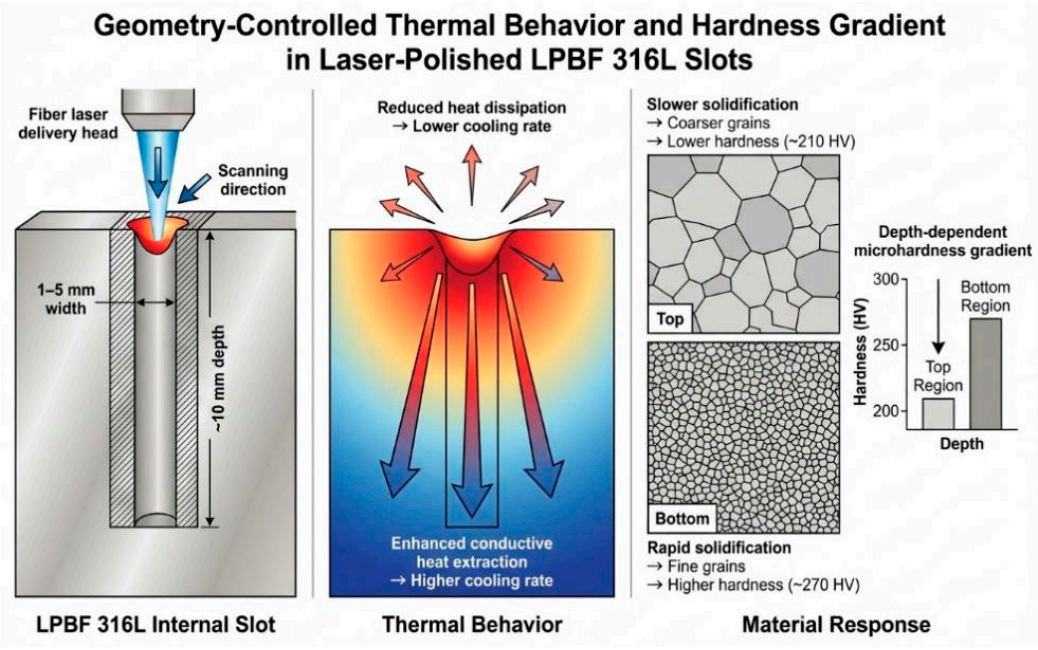

Figure 1. schematically illustrates the geometry-controlled thermal gradients in laser-polished LPBF 316L slots and their influence on microstructural evolution and hardness distribution. **Geometry-controlled thermal behavior and resulting microstructural and hardness gradients in laser-polished LPBF 316L internal slots.** Schematic illustration showing (left) the laser polishing setup applied to a narrow internal slot geometry, (middle) the associated heat transfer behavior, and (right) the resulting material response. The confined slot geometry restricts lateral heat dissipation near the top region, leading to reduced cooling rates, slower solidification, and the formation of coarser grains with lower hardness. In contrast, deeper regions experience enhanced conductive heat extraction, resulting in higher cooling rates, rapid solidification, finer grain structures,

 doi:10.20944/preprints202603.0074.v2

and increased hardness. This depth-dependent thermal gradient governs the observed microstructural variation and corresponding hardness distribution within the slot.

2. Methodology

2.1. Specimen Fabrication and Geometry

The specimens investigated in this study were fabricated from 316L stainless steel using laser powder bed fusion (LPBF). The components were specifically designed to incorporate straight internal slot geometries with a depth of approximately 10 mm and widths ranging from 1 to 5 mm. These geometrical configurations were selected to systematically investigate the influence of geometric confinement on heat transfer, microstructural evolution, and mechanical response during laser polishing. The use of well-defined slot geometries enables controlled comparison of different depth regions along the slot wall under identical processing conditions, thereby isolating the effect of geometric boundary conditions on thermal behaviour and material response.

2.2. Laser Polishing Procedure

Laser polishing was performed using a continuous-wave fibre laser operating at a wavelength of approximately 1,060–1,080 nm. The processing parameters were selected to promote stable surface remelting while avoiding excessive material removal or distortion. The laser power was maintained in the range of 80–120 W, and the scanning speed was varied between 450 and 750 mm/s. The laser beam was focused to an effective spot diameter of approximately 80–100 μm at the work surface. A raster scanning strategy was employed along the slot walls, with a track overlap of approximately 60–70% to ensure uniform surface coverage. A single-pass polishing approach was adopted for all specimens to maintain consistency across different geometries. Nitrogen shielding gas was used during processing to minimize oxidation and stabilize the melt pool. To provide a reproducible description of the processing conditions, the applied energy input was characterized using:

$$E = \frac{P}{v \cdot d}$$

where $P$is the laser power, $v$is the scan speed, and $d$is the effective beam diameter. Based on these parameters, the process operates within a controlled remelting regime suitable for modifying surface morphology and near-surface microstructure.

2.3. Metallographic Preparation and Grain Size Analysis

Following laser polishing, the specimens were sectioned to expose the internal slot walls for detailed characterization. Standard metallographic preparation procedures were employed, including sequential grinding and diamond polishing, to obtain a smooth and deformation-free surface suitable for microstructural analysis. Chemical etching was performed using aqua regia to reveal grain boundaries. Optical microscopy was used to examine the microstructure at three distinct depths along the slot wall: the lower region (~1 mm), middle region (~5 mm), and upper region (~10 mm). Grain-size measurements were performed using ImageJ software, employing thresholding and watershed segmentation techniques for accurate grain boundary detection. Quantitative grain-size values were obtained using area-based measurements and cross-validated using the linear intercept method in accordance with ASTM E112 standards. This combined approach ensures reliable and reproducible grain-size evaluation across different depth regions.

2.4. Microhardness Measurement

Microhardness measurements were conducted using a Vickers hardness tester ($HV_{0.5}$). Indentations were performed at three defined locations along the slot wall corresponding to the lower (~1 mm), middle (~5 mm), and upper (~10 mm) regions. A load of 500 g with a dwell time of 10 s was applied for each indentation. To ensure statistical reliability, five independent indentations were performed at each location, and the average value was reported. All measurements were carried out

 doi:10.20944/preprints202603.0074.v2

after laser polishing to directly evaluate the influence of thermal processing on local mechanical response. Since all specimens were fabricated under identical LPBF conditions and processed using consistent laser parameters, the observed variations are attributed primarily to geometry-dependent thermal effects rather than differences in the initial material condition.

2.5. Statistical Analysis

To evaluate the significance of the observed variations, statistical analysis was performed on both hardness and grain-size data. The reported values are expressed as mean ± standard deviation based on multiple measurements (n = 5). Differences between depth regions were assessed using one-way analysis of variance (ANOVA) with a significance level of $p < 0.05$. This confirms that the observed depth-dependent variations in hardness and microstructure are statistically significant and not attributable to experimental variability. Statistical methods such as ANOVA are widely employed in manufacturing research, including Taguchi-based and hybrid optimization approaches, to assess parameter significance and variability. In the present study, ANOVA is used to rigorously validate the significance of geometry-dependent trends observed in both microhardness and grain-size evolution.

2.6. Surface Roughness Consideration

Surface roughness is commonly used as a primary indicator of laser polishing performance. Numerous studies on LPBF-fabricated 316L stainless steel have consistently reported significant reductions in surface roughness following laser polishing, typically attributed to surface remelting and capillary-driven material redistribution [11–14]. In the present work, the primary objective is not to quantify surface finish improvement, but rather to investigate the influence of geometric confinement on thermal behaviour and the resulting microstructure–property relationship within internal features. Accordingly, the analysis focuses on depth-dependent variations in microhardness and grain size as direct indicators of local solidification behaviour. This approach enables a more fundamental understanding of geometry-driven thermal effects, which cannot be captured solely through surface roughness measurements. Therefore, while roughness reduction is an inherent outcome of laser polishing, the present study emphasizes microstructural evolution and mechanical response as more sensitive indicators of confinement-induced thermal variations.

2.7. Thermal Consideration and Simplified Model

To provide a physics-based interpretation of the observed microstructural and mechanical variations, a simplified thermal analysis is considered. The energy input during laser polishing can be described by the linear energy density:

$$E = \frac{P}{v \cdot d}$$

where P is the laser power, v is the scan speed, and d is the effective beam diameter. Under constant processing parameters, variations in material response are primarily governed by differences in heat dissipation conditions rather than changes in input energy.

The cooling rate during solidification can be approximated as proportional to the product of thermal gradient (G) and solidification velocity (R):

$$\text{Cooling rate} \propto G \times R$$

In confined slot geometries, the thermal boundary conditions vary along the depth. The lower region of the slot is in strong conductive contact with the surrounding bulk substrate, providing an efficient pathway for heat extraction. This results in a higher thermal gradient and consequently a higher effective cooling rate. In contrast, regions closer to the slot opening experience reduced conductive coupling and partial exposure to the surrounding environment, leading to comparatively lower thermal gradients and slower cooling rates. These variations in cooling behaviour directly influence grain growth and hardness development, with higher cooling rates promoting finer grain structures and increased hardness, consistent with the experimental observations. This simplified model

 doi:10.20944/preprints202603.0074.v2

provides a mechanistic framework linking geometric confinement to microstructure–property evolution during laser polishing.

2.8. Pre- and Post-Polishing Measurement Considerations

All microstructural and mechanical measurements in this study were performed after laser polishing. The primary objective was to evaluate the effect of laser-induced thermal processing on the material response within confined geometries. To ensure consistency, all specimens were fabricated from the same LPBF build under identical processing conditions, minimizing variability in the initial microstructure. Consequently, differences observed along the slot depth are attributed to geometry-dependent thermal effects during laser polishing rather than variations in the as-built condition. This approach is consistent with prior studies investigating process-induced microstructural evolution in additively manufactured materials, where controlled processing conditions allow isolation of specific variables such as geometry and thermal boundary effects.

3. Results

3.1. Geometry-Dependent Thermal Behaviour

Laser–material interaction within confined internal geometries differs significantly from open-surface conditions due to variations in heat-transfer pathways. The additively manufactured LPBF 316L specimen containing internal slots is shown in **Figure 2a**, while a schematic representation of laser polishing within the slot geometry is illustrated in **Figure 2b**. The slot walls, spaced 1–5 mm apart and extending to a depth of approximately 10 mm, provide a controlled framework for evaluating geometry-dependent thermal effects. Laser polishing was performed using a continuous-wave fibre laser ($\lambda \approx 1{,}060$–$1{,}080$ nm) at powers of 80–120 W and scan speeds of 450–750 mm/s, with nitrogen shielding gas employed to stabilize the melt pool and minimize oxidation. Within these confined geometries, the thermal boundary conditions vary along the slot height due to differences in conductive and environmental heat dissipation, as conceptually illustrated in **Figure 3**. The lower region of the slot is in direct conductive contact with the surrounding bulk substrate, providing an efficient pathway for heat extraction into the underlying material. In contrast, regions closer to the slot opening experience reduced conductive coupling and partial exposure to the surrounding environment, resulting in modified heat dissipation characteristics. As a result, depth-dependent variations in cooling behaviour are established during laser polishing. The lower region, which is more strongly coupled to the bulk material, undergoes enhanced conductive heat extraction and consequently higher effective cooling rates following laser interaction. Toward the upper region, where conductive pathways differ and environmental exposure becomes more significant, the effective cooling rate is comparatively reduced. This geometry-dependent variation in thermal extraction becomes more pronounced as slot width decreases, since narrower geometries restrict lateral heat flow and constrain melt-pool dimensions. Consequently, the observed microstructural evolution and hardness gradients along the slot wall are consistent with these depth-dependent thermal conditions, confirming the strong influence of geometric confinement on thermal behaviour during laser polishing.

 doi:10.20944/preprints202603.0074.v2

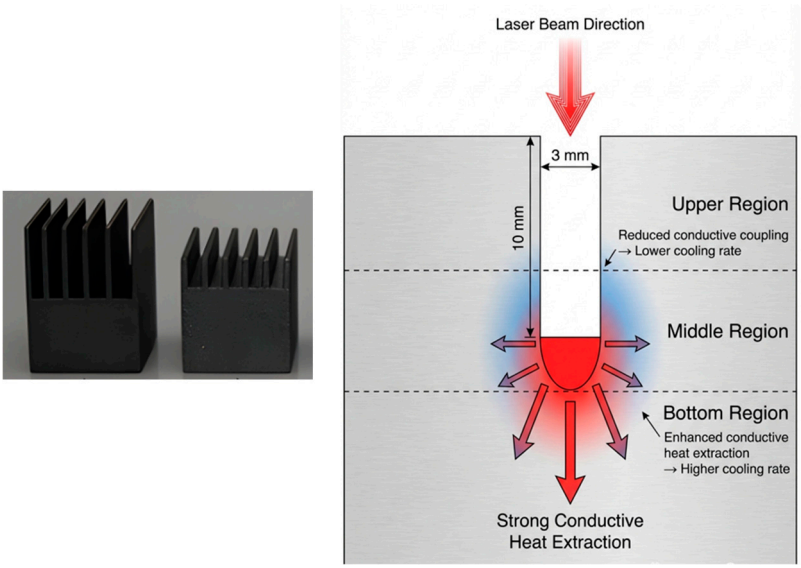

(**a**) (**b**)

Figure 2. (a) Photograph of the additively manufactured LPBF 316L stainless steel specimen containing internal slots used for laser polishing experiments; **(b)** Schematic illustration of laser polishing within a narrow internal slot (1–5 mm width, ~10 mm depth), showing geometry-dependent heat extraction during processing. Note: The lower region of the slot is in direct conductive contact with the surrounding bulk substrate, promoting enhanced heat extraction and relatively higher cooling rates following laser passage. Toward the slot opening, conductive coupling differs due to geometric boundary conditions and environmental exposure, resulting in comparatively lower cooling rates. These depth-dependent variations in thermal behaviour influence solidification conditions, grain evolution, and the resulting microhardness Gradient observed along the polished slot wall.

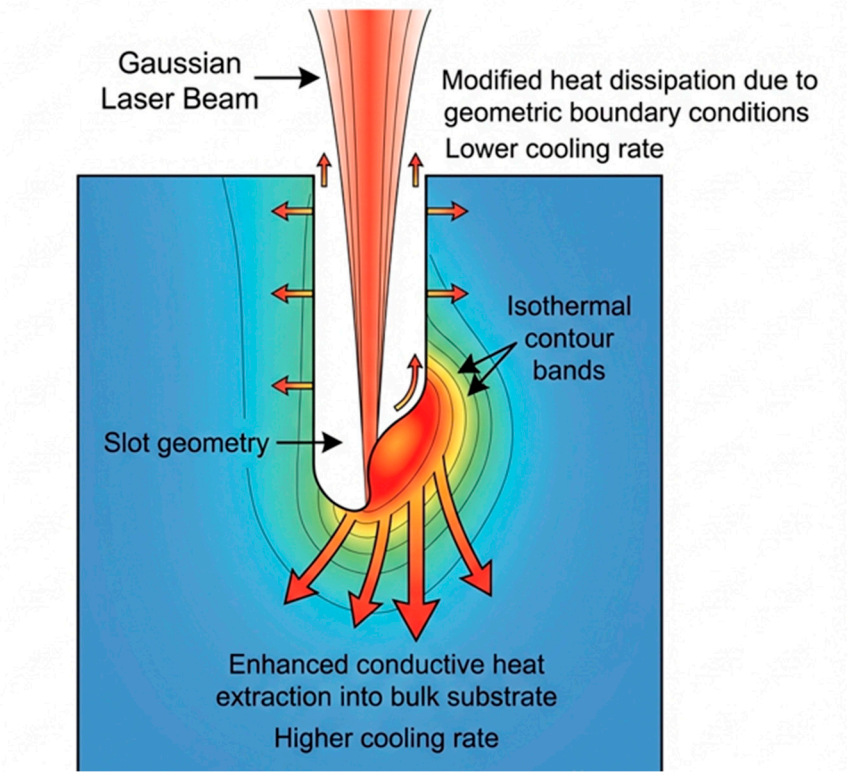

Figure 3. Schematic representation of heat transfer during laser polishing inside a narrow internal slot. Note: The Gaussian laser beam generates a localized heat source along the slot wall. Due to geometric boundary conditions, heat extraction varies along the slot depth. The lower region is in strong conductive contact with the surrounding bulk substrate, promoting enhanced heat extraction and relatively higher cooling rates. Toward the slot opening, heat dissipation conditions differ due to altered conductive pathways and environmental exposure,

 doi:10.20944/preprints202603.0074.v2

resulting in comparatively lower cooling rates. The isothermal contour bands illustrate the depth-dependent thermal field established during processing.

3.2. Depth-Resolved Microhardness Gradient

To quantify the mechanical response associated with geometry-dependent heat extraction, Vickers micro-indentation hardness ($HV_{0.5}$) measurements were performed at three defined depths along the slot wall: the lower region (~1 mm from the polished surface), the middle region (~5 mm), and the upper region (~10 mm). Five independent indentations were obtained at each depth, and the mean values with corresponding variability are presented in **Figure 4**. Across all slot widths (1–4 mm), a consistent decrease in hardness with increasing height along the slot wall was observed. For instance, in the 3 mm slot, hardness decreases from approximately 271 HV in the lower region to about 249 HV in the upper region. Similar depth-dependent trends are evident across the other geometries, indicating a systematic and reproducible gradient in mechanical response. This behaviour is consistent with the geometry-dependent thermal conditions described in Subsection 3.1. The lower region, which is in stronger conductive contact with the bulk substrate, experiences enhanced heat extraction and consequently higher effective cooling rates following laser interaction. In contrast, regions closer to the slot opening exhibit comparatively reduced cooling rates due to altered thermal boundary conditions. The observed hardness variation is closely correlated with the corresponding grain-size differences discussed in Subsection 3.3, where finer grains in the lower region are associated with higher hardness, while coarser grains toward the upper region correspond to reduced hardness. This relationship is consistent with established microstructure–property principles governing solidification-controlled grain evolution. Overall, the results demonstrate a clear and consistent relationship between slot geometry, depth position, and microhardness evolution under constant processing parameters, highlighting the significant influence of geometric confinement on local mechanical response during laser polishing.

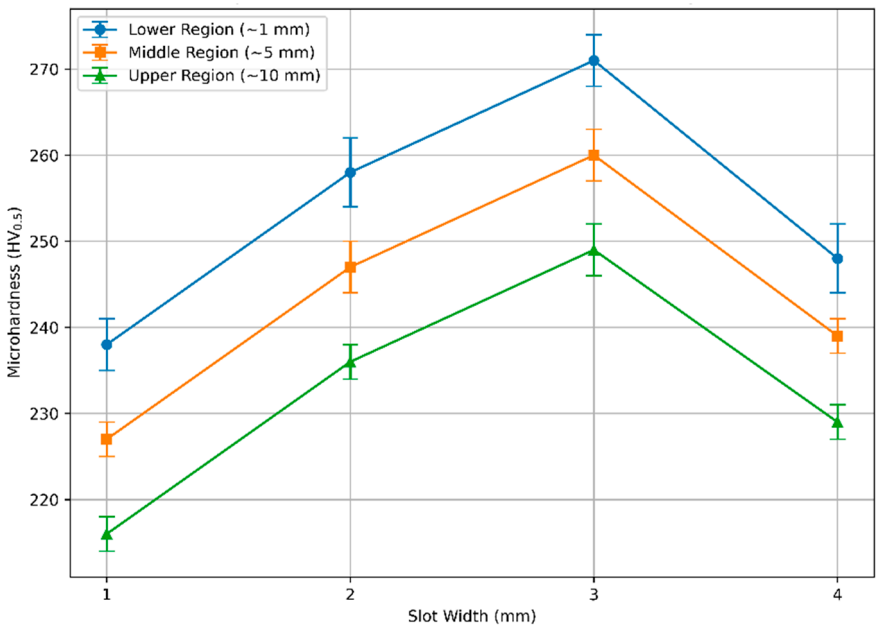

Figure 4. Depth-resolved microhardness of the laser-polished slot wall measured at the lower (~1 mm), middle (~5 mm), and upper (~10 mm) regions for slot widths of 1–4 mm. Note: Error bars represent mean ± standard deviation (n = 5). A consistent decrease in hardness with increasing height along the slot wall is observed across all geometries. The lower region exhibits the highest hardness, followed by the middle and upper regions. This systematic gradient is consistent with depth-dependent variations in cooling behaviour during laser polishing, where enhanced conductive heat extraction near the lower region promotes comparatively higher cooling rates

 doi:10.20944/preprints202603.0074.v2

and finer grain structures, while regions closer to the slot opening experience comparatively lower cooling rates and reduced hardness.

The depth-resolved microhardness values summarized in **Table 1** further confirm the systematic variation in mechanical response along the slot wall. The lower region consistently exhibits the highest hardness, followed by the middle and upper regions across all slot widths. For example, in the 3 mm slot, hardness decreases from 271 HV in the lower region to 249 HV in the upper region, consistent with the trend observed in **Figure 4**. This depth-dependent behaviour is consistently observed for all geometries presented in **Table 1**, indicating a robust and reproducible gradient in hardness along the slot depth. The observed trend is closely linked to geometry-dependent heat extraction during laser polishing. The lower region of the slot, being in strong conductive contact with the surrounding bulk substrate, facilitates efficient heat dissipation and consequently experiences higher effective cooling rates following laser interaction. In contrast, regions closer to the slot opening exhibit reduced conductive coupling and modified thermal boundary conditions, resulting in comparatively lower cooling rates. These variations in cooling behaviour directly correlate with the grain-size differences discussed in Subsection 3.3. According to Hall–Petch behaviour, finer grain structures contribute to higher hardness, whereas coarser grains lead to reduced hardness. Furthermore, the magnitude of the hardness difference between the lower and upper regions ($\Delta HV = HV\_lower - HV\_upper$) varies with slot width, as evident from **Table 1**. Slots in the 1–3 mm range exhibit relatively larger ΔHV values compared to the 4 mm slot, suggesting that intermediate geometries promote more pronounced depth-dependent thermal gradients under the present processing conditions. This observation reinforces the role of geometric confinement in governing local cooling behaviour and mechanical response during laser polishing.

Table 1. Depth-resolved microhardness values (mean $HV_{0.5}$) for slot widths of 1–4 mm.

Slot width (mm)	Lower HV	Middle HV	Upper HV
1	238	227	216
2	258	247	236
3	271	260	249
4	248	239	229

3.3. Microstructure Evolution

Optical micrographs of the laser-polished slot walls reveal clear depth-dependent variations in grain morphology. The specimens were prepared using standard metallographic procedures, including grinding and diamond polishing, followed by etching with aqua regia to delineate grain boundaries for quantitative analysis. Grain-size measurements were carried out using ImageJ, employing thresholding and watershed segmentation techniques for accurate grain boundary detection and area-based quantification. The results were further validated using the linear intercept method in accordance with ASTM E112 standards, with good agreement observed between the two approaches. As shown in **Figure 4**, the lower region of the slot exhibits finer and more uniformly distributed equiaxed grains compared to the middle and upper regions, whereas the upper region is characterized by comparatively coarser grain structures. This systematic variation in grain morphology is consistent with the depth-dependent thermal behaviour described in Subsection 3.1. The lower region, being in stronger conductive contact with the surrounding bulk substrate, facilitates enhanced heat extraction and consequently experiences higher effective cooling rates following laser interaction. In contrast, regions nearer the slot opening exhibit reduced conductive coupling and altered thermal boundary conditions, resulting in comparatively lower cooling rates. These differences in cooling behaviour directly influence solidification dynamics and grain growth. Higher cooling rates in the lower region promote grain refinement, while reduced cooling rates toward the upper region allow for increased grain growth and coarsening. The observed microstructural trends are therefore consistent with fundamental solidification principles governing

 doi:10.20944/preprints202603.0074.v2

thermally driven microstructure evolution. Furthermore, the grain-size variation correlates closely with the hardness trends discussed in Subsection 3.2. According to the Hall–Petch relationship, finer grains contribute to increased hardness, whereas coarser grains lead to reduced hardness. The combined microstructural and mechanical results therefore establish a clear and consistent depth-dependent microstructure–property relationship within the laser-polished slot geometry.

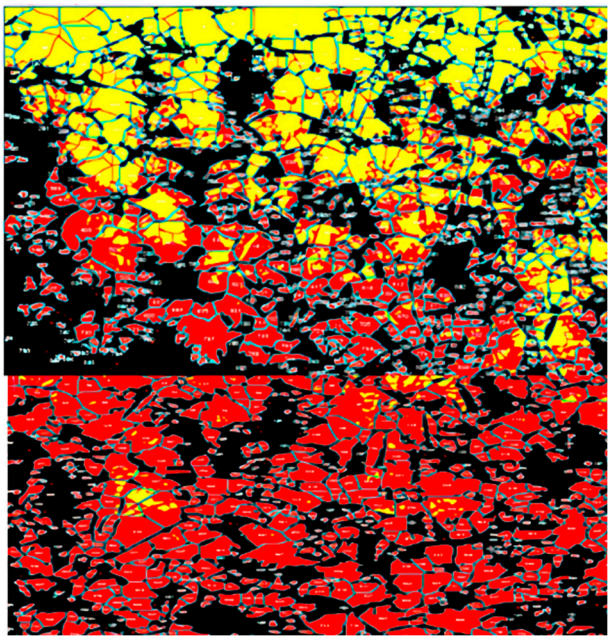

(**a**)

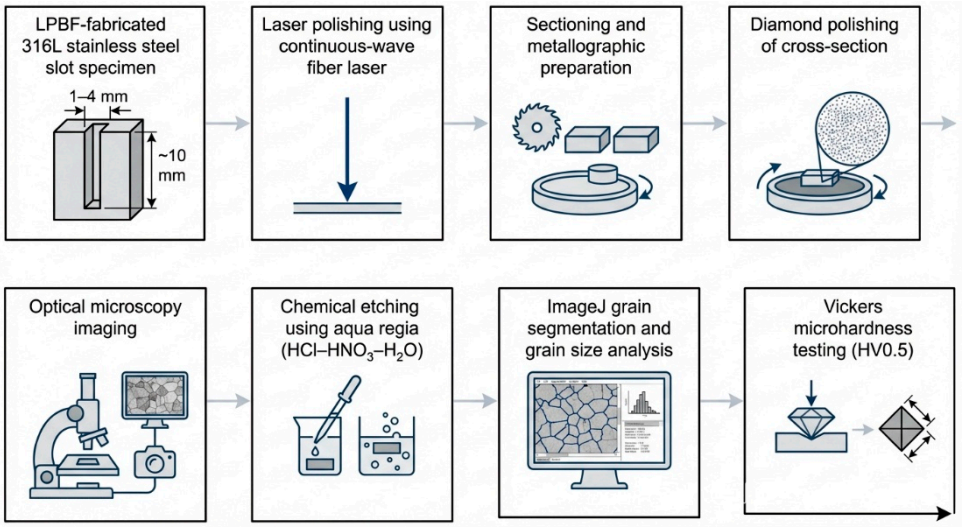

(**b**)

Figure 5. (a) ImageJ-assisted grain segmentation of optical micrographs from the laser-polished 316L slot wall after metallographic preparation and aqua regia etching. (b) Schematic of the workflow: LPBF fabrication, laser polishing, sectioning, metallographic and diamond polishing, etching, optical microscopy, ImageJ segmentation, and Vickers microhardness testing ($HV_{0.5}$). Note: **Figure 5a**: The upper portion corresponds to the lower region (~1 mm from the polished surface), and the lower portion to the upper region (~10 mm). Grain boundaries were identified using thresholding and watershed segmentation, and grain sizes were measured using area-based methods, cross-validated by the linear intercept method (ASTM E112). Finer grains are observed in the lower region, while coarser grains appear toward the slot opening, consistent with hardness variation (**Figure 4**) and Hall–Petch behaviour.

 doi:10.20944/preprints202603.0074.v2

3.4. Combined Surface Roughness and Hardness Evolution

A combined summary of representative surface roughness and microhardness values before and after laser polishing is presented in **Table 2**. In the as-built condition, the material exhibits relatively uniform hardness (≈220–245 $HV_{0.5}$) along with moderate surface roughness values (≈5.2–6.2 μm), which are typical for LPBF-fabricated 316L stainless steel. Following laser polishing, a clear improvement in surface quality is observed across all geometries, with roughness values decreasing to approximately 1.9–3.4 μm. This reduction is attributed to localized surface remelting and capillary-driven material flow, which smoothens surface irregularities formed during the additive manufacturing process. At the same time, a distinct depth-dependent variation in hardness emerges after polishing. As shown in **Table 2**, the lower regions exhibit increased hardness compared to the pre-polishing condition, whereas the upper regions show comparatively lower hardness values. This indicates that laser polishing not only enhances surface morphology but also modifies the near-surface microstructure through remelting and subsequent solidification. While the reduction in surface roughness is relatively consistent across different slot widths, the variation in hardness is strongly influenced by geometry-dependent thermal conditions. Enhanced heat extraction in the lower regions leads to higher cooling rates and grain refinement, whereas reduced thermal dissipation near the slot opening results in comparatively lower hardness. Overall, these results demonstrate that laser polishing induces both surface and subsurface modifications. The inclusion of pre-polishing baseline values confirms that the observed hardness gradients are a direct consequence of geometry-dependent thermal effects during laser processing, rather than variations in the initial material condition.

Table 2. Representative surface roughness (Ra, μm) and microhardness ($HV_{0.5}$) before and after laser polishing.

Slot width (mm)	Pre-Ra (μm)	Post-Ra (μm)	Pre-$HV_{0.5}$	Post-$HV_{0.5}$ (lower)	Post-$HV_{0.5}$ (upper)
1	6.2 ± 0.6	3.4 ± 0.3	220 ± 5	238 ± 4	216 ± 3
2	5.8 ± 0.5	2.6 ± 0.2	235 ± 6	258 ± 5	236 ± 4
3	5.5 ± 0.5	1.9 ± 0.2	245 ± 5	271 ± 4	249 ± 4
4	5.2 ± 0.4	2.3 ± 0.3	240 ± 5	248 ± 4	229 ± 3

4. Discussion

4.1. Mechanistic Interpretation

The results clearly show that the mechanical response of laser-polished internal slots is strongly governed by geometry-dependent thermal boundary conditions. During laser polishing, localized surface remelting occurs along the slot wall, followed by rapid solidification controlled by the available heat extraction pathways. This remelting-driven process, rather than solid-state heating, is responsible for the observed microstructural and mechanical evolution. For the slot geometries examined (1–4 mm width and ~10 mm depth), the lower region of the slot remains in direct conductive contact with the surrounding bulk substrate. This provides an efficient pathway for heat dissipation, leading to relatively higher cooling rates after laser interaction. In contrast, regions closer to the slot opening experience reduced conductive coupling and greater exposure to the surrounding environment, resulting in modified thermal boundary conditions and comparatively lower cooling rates. The depth-resolved hardness trends shown in **Figure 4** reflect this behaviour, with hardness decreasing consistently from the lower to the upper region. Correspondingly, the microstructural observations presented in Subsection 3.3 reveal finer grains in the lower region and coarser grains toward the upper region, which is consistent with cooling-rate-dependent solidification. According to the Hall–Petch relationship, smaller grain sizes contribute to increased hardness, establishing a direct link between thermal extraction behaviour and mechanical response. The influence of geometry is further evident in the variation of hardness with slot width. Slots in the 1–3 mm range

 doi:10.20944/preprints202603.0074.v2

exhibit relatively larger hardness differences between the lower and upper regions, whereas the 4 mm slot shows a reduced gradient. This non-monotonic behaviour suggests that intermediate slot widths provide a balance between conductive heat extraction into the substrate and lateral heat dissipation along the slot walls under the present processing conditions. The hardness difference between the lower and upper regions (ΔHV), as shown in **Figure 6**, further highlights the geometry-dependent nature of the thermal effects. Since laser power and scan speed were kept constant, these variations can be attributed primarily to differences in heat dissipation conditions rather than changes in processing parameters. Although direct thermal measurements were not performed, the strong agreement between hardness trends and grain-size evolution provides consistent indirect evidence of depth-dependent cooling behaviour. Overall, these findings demonstrate that geometric boundary conditions play a critical role in governing microstructure–property relationships during laser polishing of confined internal features.

Figure 6. Variation of hardness difference (ΔHV = HV_lower − HV_upper) as a function of slot width. Note: Error bars represent propagated uncertainty from individual hardness measurements (mean ± standard deviation). The hardness differential remains relatively consistent for slot widths of 1–3 mm and decreases for the 4 mm slot. This behaviour indicates that the magnitude of the depth-dependent hardness gradient is influenced by slot geometry under constant processing conditions. The trend highlights the geometry-dependent nature of thermal effects during laser polishing without implying a strictly linear or monotonic relationship.

4.2. Engineering Relevance

The findings of this study are directly relevant to engineering applications involving internal channels, narrow features, and complex three-dimensional geometries. In biomedical engineering, laser-polished internal surfaces in implants and surgical instruments require controlled surface integrity and consistent mechanical response. Understanding how geometric boundary conditions influence cooling behaviour during laser polishing provides a pathway for improving the reliability and uniformity of internal surface properties. In microscale heat exchangers and metal microfluidic systems, internal wall characteristics significantly affect flow resistance, heat transfer efficiency, and structural durability. The present results demonstrate that internal geometry can influence local microstructure and hardness following laser polishing, highlighting the need to account for geometric confinement during both design and post-processing stages. Similarly, aerospace cooling passages and additively manufactured turbine components operate under demanding thermomechanical conditions, where internal surface integrity is critical. The observed depth-dependent hardness variations indicate that geometry can influence local solidification behaviour

 doi:10.20944/preprints202603.0074.v2

during polishing, potentially affecting component reliability under service conditions. Recognizing such geometry–process interactions enables more informed design strategies aimed at achieving either uniform properties or intentionally graded material behaviour, depending on application requirements.

4.3. Innovation and Impact

This study demonstrates that internal geometry can significantly influence the mechanical response of laser-polished features, even when nominal processing parameters are held constant. The experimentally observed depth-dependent gradients in hardness and grain structure reveal a geometry–process interaction that has received limited systematic attention in confined additively manufactured features. The results show that geometric boundary conditions influence cooling behaviour during solidification, thereby governing the resulting microstructure–property relationship. Although direct thermal measurements were not performed, the strong correlation between grain size and hardness supports a Hall–Petch-type interpretation of the observed gradients. From a design perspective, these findings highlight the importance of incorporating geometric effects into process optimization strategies for laser polishing. Adjustments in feature dimensions or processing conditions may be used to reduce property gradients or tailor local mechanical response based on application requirements.

4.4. Comparison with Existing Literature

The observed hardness values (approximately 210–270 HV) and grain-size ranges (≈8–25 μm) are consistent with previously reported data for LPBF-fabricated and laser-processed 316L stainless steel [7,10,11]. Prior studies have shown that higher cooling rates during laser processing promote grain refinement and increased hardness, while reduced cooling rates lead to grain coarsening and lower hardness, as supported by both experimental observations and numerical simulations of melt-pool behaviour [5,7,38]. The trends observed in this study finer grains and higher hardness in regions with enhanced heat extraction, and coarser grains with reduced hardness in regions of limited thermal dissipation are in strong agreement with established findings in laser-based additive manufacturing and post-processing studies, where thermal gradients and solidification dynamics govern microstructure evolution [4,26,38]. However, unlike most existing studies that primarily focus on open surfaces, melt-pool cross-sections, or bulk material behaviour, the present work provides direct experimental evidence of depth-dependent microstructure–property variation within confined internal geometries. While previous investigations have explored internal channel polishing and geometry effects, they have largely emphasized surface quality rather than depth-resolved mechanical and microstructural gradients [2,3,15]. Therefore, this study extends current understanding by demonstrating that geometric confinement introduces spatially varying thermal boundary conditions, which in turn influence local cooling rates, grain evolution, and hardness. These findings reinforce the importance of explicitly considering geometry-dependent heat-transfer effects when interpreting and optimizing laser polishing processes for additively manufactured components.

4.5. Dimensional and Tolerance Considerations

The laser polishing process in this study was conducted within a controlled remelting regime, with process parameters carefully selected to minimize excessive material removal and avoid geometric distortion. Throughout the experiments, no noticeable macroscopic deformation or dimensional deviation was observed in the polished slot geometries. This indicates that the process preserves the dimensional integrity and tolerances of the internal features while modifying only the near-surface microstructure. Consequently, the observed microhardness gradients and grain-size variations can be attributed to thermally driven microstructural evolution rather than any changes in geometry or dimensional instability. These findings confirm that laser polishing can be effectively

 doi:10.20944/preprints202603.0074.v2

applied to confined internal geometries without compromising dimensional accuracy. This is particularly important for engineering applications requiring tight tolerances, such as aerospace cooling channels, precision microfluidic systems, and biomedical components.

4.6. Effect of Metallographic (Diamond) Polishing

The diamond polishing step employed in this study was performed solely for metallographic preparation after sectioning the specimens. Its purpose was to obtain a smooth, deformation-free surface suitable for accurate microstructural observation and microhardness measurement. Importantly, this preparation step does not alter the intrinsic microstructure generated by the laser polishing process. Since it is applied after sectioning and does not involve thermal input or phase transformation, it does not introduce microstructural modifications within the material. Therefore, the observed grain morphology and hardness variations are representative of the actual laser-polished condition and are not artefacts arising from sample preparation. This ensures that the reported microstructure–property relationships accurately reflect the effects of laser polishing under the investigated processing conditions.

5. Limitations and Future Directions

Several limitations define the scope of the present study and also highlight important directions for future research.

First, the experiments were conducted on straight rectangular slot geometries (1–4 mm width and ~10 mm depth). While this configuration effectively captures key aspects of confined laser polishing conditions, real engineering components often incorporate more complex internal features such as curved, tapered, or branched channels. Extending the analysis to such geometries would provide a more comprehensive understanding of geometry-dependent thermal behaviour and its influence on microstructure and mechanical response.

Second, the mechanical response in this study was primarily evaluated through microhardness and grain-size measurements. Although these metrics are well-established indicators of near-surface strengthening and microstructural evolution, additional characterization such as fatigue performance, corrosion resistance, and wear behaviour would further enhance the application-level relevance of the findings.

Third, direct thermal measurements and numerical modelling were not included in the present work. While the observed trends are supported by consistent microstructure–property correlations, incorporating validated transient heat-transfer simulations and in situ temperature measurements would enable quantitative prediction of cooling rates and thermal gradients, thereby strengthening the mechanistic interpretation.

Finally, the study was performed using a continuous-wave fibre laser within a defined parameter range. Exploring alternative laser modes, scanning strategies, and broader energy input conditions may offer additional opportunities to tailor microstructure and mechanical properties within confined internal features. These limitations do not detract from the central finding that internal geometry plays a critical role in governing microstructure and hardness during laser polishing. Instead, they establish a foundation for future work aimed at integrating experimental characterization, thermal modelling, and application-driven design strategies for advanced additively manufactured systems.

6. Conclusions

This study systematically investigated the influence of internal slot geometry on the microstructural and mechanical response of laser-polished additively manufactured 316L stainless steel. For slot widths ranging from 1 to 4 mm and a depth of approximately 10 mm, a clear depth-dependent microhardness gradient was observed, with the lower regions consistently exhibiting higher hardness than the middle and upper regions. These variations in hardness were found to

 doi:10.20944/preprints202603.0074.v2

correlate directly with corresponding changes in grain morphology, where finer grains were observed in the lower regions and comparatively coarser grains toward the slot opening. This behaviour is attributed to geometry-dependent thermal boundary conditions during laser polishing, where enhanced conductive heat extraction in the lower region results in higher cooling rates, while reduced thermal dissipation near the slot opening leads to slower solidification. The observed relationship between grain refinement and increased hardness is consistent with established Hall–Petch principles, confirming a strong microstructure–property linkage governed by cooling-rate variation. Importantly, these results demonstrate that internal geometry can significantly influence local microstructure and mechanical response even when nominal laser processing parameters are held constant. From a broader perspective, the findings highlight the critical role of geometric confinement in governing thermal behaviour and material response during laser polishing. This geometry–process interaction underscores the need to explicitly consider feature dimensions and boundary conditions during the design and post-processing of additively manufactured components. The insights gained from this study are particularly relevant for applications involving confined internal features, such as biomedical devices, aerospace cooling channels, and compact thermal systems. Incorporating geometry-dependent effects into process optimization strategies can enable improved control over local material properties, leading to more reliable and functionally optimized components.

Funding: This research was conducted without any external financial support or funding.

Institutional review board statement: Not applicable.

Informed consent statement: Not applicable.

Data aavailabilityy statement: All datasets and analysis scripts used in this study were generated directly from the documented methods and parameters. They are fully reproducible and are available from the author upon reasonable request.

Acknowledgments: The author gratefully acknowledges the laboratory facilities and technical assistance provided during the course of this work. The author also extends sincere thanks to colleagues and mentors whose guidance and general support contributed to the successful completion of this research.

Conflicts of Interest: The author declares that there are no conflicts of interest associated with this work.

AI use statement: The author used AI-assisted language editing tools (Grammarly) solely for improving grammar, clarity, and readability. All scientific content, analysis, and interpretations were developed independently by the author.

References

1. Siddiqui AA, Dubey AK. Recent trends in laser cladding and surface alloying. Optics & Laser Technology. 2021; 134: 106619. doi: 10.1016/j.optlastec.2020.106619
2. Khan SA, Shamail S, Anwar S, et al. Wear performance of surface treated drills in high speed drilling of AISI 304 stainless steel. Journal of Manufacturing Processes. 2020; 58: 223–235. doi: 10.1016/j.jmapro.2020.08.022
3. Guo J, Xiang C, Rossiter J. A soft and shape-adaptive electroadhesive composite gripper with proprioceptive and exteroceptive capabilities. Materials & Design. 2018; 156: 586–587. doi: 10.1016/j.matdes.2018.07.027
4. DebRoy T, Wei HL, Zuback JS, et al. Additive manufacturing of metallic components – Process, structure and properties. Progress in Materials Science. 2018; 92: 112–224. doi: 10.1016/j.pmatsci.2017.10.001
5. Chandran AM, Varun S, Bhargavi PVB, et al. h-BN and graphene oxide/epoxy nanocomposite—A comparative study of mechanical, electrical and thermal properties. In: Proceedings of the Fracture and Damage Mechanics: Theory, Simulation and Experiment; 15–17 September 2020; Mallorca, Spain, p. 020002. doi: 10.1063/5.0028259

 doi:10.20944/preprints202603.0074.v2

6. King WE, Barth HD, Castillo VM, et al. Observation of keyhole-mode laser melting in laser powder-bed fusion additive manufacturing. Journal of Materials Processing Technology. 2014; 214(12): 2915–2925. doi: 10.1016/j.jmatprotec.2014.06.005
7. Li W, Yamasaki S, Mitsuhara M, et al. In situ EBSD study of deformation behavior of primary α phase in a bimodal Ti-6Al-4V alloy during uniaxial tensile tests. Materials Characterization. 2020; 163: 110282. doi: 10.1016/j.matchar.2020.110282
8. Schneider CA, Rasband WS, Eliceiri KW. NIH Image to ImageJ: 25 years of image analysis. Nature Methods. 2012; 9(7): 671–675. doi: 10.1038/nmeth.2089
9. ASTM. Standard Test Methods for Determining Average Grain Size. ASTM International; 2004.
10. Hamza HM, Deen KM, Khaliq A, et al. Microstructural, corrosion and mechanical properties of additively manufactured alloys: A review. Critical Reviews in Solid State and Materials Sciences. 2022; 47(1): 46–98. doi: 10.1080/10408436.2021.1886044
11. Chen L, Richter B, Zhang X, et al. Modification of surface characteristics and electrochemical corrosion behavior of laser powder bed fused stainless-steel 316L after laser polishing. Additive Manufacturing. 2020; 32: 101013. doi: 10.1016/j.addma.2019.101013
12. Obeidi MA, McCarthy E, O'Connell B, et al. Laser Polishing of Additive Manufactured 316L Stainless Steel Synthesized by Selective Laser Melting. Materials. 2019; 12(6): 991. doi: 10.3390/ma12060991
13. Jiang Z, Song B, Zhou X, et al. On-machine measurement of location errors on five-axis machine tools by machining tests and a laser displacement sensor. International Journal of Machine Tools and Manufacture. 2015; 95: 1–12. doi: 10.1016/j.ijmachtools.2015.05.004
14. Lamikiz A, Sánchez JA, López De Lacalle LN, et al. Laser polishing of parts built up by selective laser sintering. International Journal of Machine Tools and Manufacture. 2007; 47(12–13): 2040–2050. doi: 10.1016/j.ijmachtools.2007.01.013
15. Manco E, Cozzolino E, Astarita A. Laser polishing of additively manufactured metal parts: A review. Surface Engineering. 2022; 38(3): 217–233. doi: 10.1080/02670844.2022.2072080
16. Adebiyi DI, Popoola API, Pityana SL. Phase constituents and microhardness of laser alloyed Ti–6Al–4 V alloy. Journal of Laser Applications. 2015; 27(S2): S29104. doi: 10.2351/1.4906388
17. Lin X, Huang WD. Laser additive manufacturing of high-performance metal components. Chinese Science: Information Science. 2015; 45(9): 1111–1126.
18. Chen J, Hou W, Wang X, et al. Microstructure, porosity and mechanical properties of selective laser melted AlSi10Mg. Chinese Journal of Aeronautics. 2020; 33(7): 2043–2054. doi: 10.1016/j.cja.2019.08.017
19. Song J, Wu W, Zhang L, et al. Role of scanning strategy on residual stress distribution in Ti-6Al-4V alloy prepared by selective laser melting. Optik. 2018; 170: 342–352. doi: 10.1016/j.ijleo.2018.05.128
20. Galy C, Le Guen E, Lacoste E, et al. Main defects observed in aluminum alloy parts produced by SLM: From causes to consequences. Additive Manufacturing. 2018; 22: 165–175. doi: 10.1016/j.addma.2018.05.005
21. Karkadakattil A. AI and Metaheuristic Optimization in Additive Manufacturing of Lightweight Alloys: A Critical Review. Journal of The Institution of Engineers (India): Series C. 2026; 107(2): 1063–1085. doi: 10.1007/s40032-026-01355-4
22. Satterlee N, Torresani E, Olevsky E, et al. Comparison of machine learning methods for automatic classification of porosities in powder-based additive manufactured metal parts. The International Journal of Advanced Manufacturing Technology. 2022; 120(9–10): 6761–6776. doi: 10.1007/s00170-022-09141-z
23. Babamiri BB, Indeck J, Demeneghi G, et al. Quantification of porosity and microstructure and their effect on quasi-static and dynamic behavior of additively manufactured Inconel 718. Additive Manufacturing. 2020; 34: 101380. doi: 10.1016/j.addma.2020.101380
24. Ge J, Pillay S, Ning H. Post-Process Treatments for Additive-Manufactured Metallic Structures: A Comprehensive Review. Journal of Materials Engineering and Performance. 2023; 32(16): 7073–7122. doi: 10.1007/s11665-023-08051-9
25. Dalpadulo E, Pini F, Leali F. Powder bed fusion integrated product and process design for additive manufacturing: a systematic approach driven by simulation. The International Journal of Advanced Manufacturing Technology. 2024; 130(11–12): 5425–5440. doi: 10.1007/s00170-024-13042-8

 doi:10.20944/preprints202603.0074.v2

26. Ding R, Yao J, Du B, et al. Effect of Shielding Gas Volume Flow on the Consistency of Microstructure and Tensile Properties of 316L Manufactured by Selective Laser Melting. Metals. 2021; 11(2): 205. doi: 10.3390/met11020205
27. Ren L, Wang N, Wang X, et al. Modeling and analysis of material removal depth contour for curved-surfaces abrasive belt grinding. Journal of Materials Processing Technology. 2023; 316: 117945. doi: 10.1016/j.jmatprotec.2023.117945
28. Du Plessis A, Yadroitsava I, Yadroitsev I. Effects of defects on mechanical properties in metal additive manufacturing: A review focusing on X-ray tomography insights. Materials & Design. 2020; 187: 108385. doi: 10.1016/j.matdes.2019.108385
29. Martin AA, Calta NP, Khairallah SA, et al. Dynamics of pore formation during laser powder bed fusion additive manufacturing. Nature Communications. 2019; 10(1): 1987. doi: 10.1038/s41467-019-10009-2
30. Yonehara M, Kato C, Ikeshoji T-T, et al. Correlation between surface texture and internal defects in laser powder-bed fusion additive manufacturing. Scientific Reports. 2021; 11(1): 22874. doi: 10.1038/s41598-021-02240-z
31. Srivastava AK, Kumar A, Kumar P, et al. Research Progress in metal additive manufacturing: Challenges and Opportunities. International Journal on Interactive Design and Manufacturing (IJIDeM). 2023; doi: 10.1007/s12008-023-01661-6
32. Karkadakattil A. A Physics-Stabilized Self-Updating Digital Twin Framework Using Physics-Informed Neural Networks for Thermal Field Prediction. Applied Computer Systems. 2026; 31(1): 30–40. doi: 10.2478/acss-2026-0003
33. Karkadakattil A. Geometry aware laser polishing of LPBF AlSi10Mg defence components with physics inspired neural network based surface roughness prediction. Discover Mechanical Engineering. 2025; 4(1): 52. doi: 10.1007/s44245-025-00144-0
34. Karkadakattil A. Physics-informed machine learning framework for grain size prediction in laser-processed 316L stainless steel: integration of experimental microstructure and surrogate data. Canadian Metallurgical Quarterly. 2025; 1–14. doi: 10.1080/00084433.2025.2593051
35. Karkadakattil A. AI-Driven prediction of surface roughness in laser-polished LPBF Ti6Al4V: a sustainable proof-of-concept. Australian Journal of Multi-Disciplinary Engineering. 2025; 1–13. doi: 10.1080/14488388.2025.2570030
36. Grasso M, Colosimo BM. Process defects and in situ monitoring methods in metal powder bed fusion: a review. Measurement Science and Technology. 2017; 28(4): 044005. doi: 10.1088/1361-6501/aa5c4f
37. Li R, Zhu J, Zhou W, et al. Thermal properties of sodium nitrate-expanded vermiculite form-stable composite phase change materials. Materials & Design. 2016; 104: 190–196. doi: 10.1016/j.matdes.2016.05.039
38. Möller F, Grden M, Thomy C, et al. Combined Laser Beam Welding and Brazing Process for Aluminium Titanium Hybrid Structures. Physics Procedia. 2011; 12: 215–223. doi: 10.1016/j.phpro.2011.03.028
39. Shin WS, Lee T, Sohn H, et al. Microstructural and mechanical properties degradation of the acceleration/deceleration zones in stainless steel 316L fabricated by selective laser melting. Journal of Materials Research and Technology. 2025; 35: 2215–2225. doi: 10.1016/j.jmrt.2025.01.183
40. Jurca M, Langer H-J. Temperature field measurement as quality assurance measure in case of laser material processing. Physics Procedia. 2010; 5: 473–481. doi: 10.1016/j.phpro.2010.08.075
41. Zhang D, Qiu D, Gibson MA, et al. Additive manufacturing of ultrafine-grained high-strength titanium alloys. Nature. 2019; 576(7785): 91–95. doi: 10.1038/s41586-019-1783-1
42. Gu D, Shen Y. Balling phenomena in direct laser sintering of stainless steel powder: Metallurgical mechanisms and control methods. Materials & Design. 2009; 30(8): 2903–2910. doi: 10.1016/j.matdes.2009.01.013
43. Childs THC, Hauser C, Badrossamay M. Selective laser sintering (melting) of stainless and tool steel powders: Experiments and modelling. Proceedings of the Institution of Mechanical Engineers, Part B: Journal of Engineering Manufacture. 2005; 219(4): 339–357. doi: 10.1243/095440505 × 8109

 doi:10.20944/preprints202603.0074.v2

44. Amini S, Amiri MR. Study of ultrasonic vibrations' effect on friction stir welding. The International Journal of Advanced Manufacturing Technology. 2014; 73(1–4): 127–135. doi: 10.1007/s00170-014-5806-7
45. Xiao X, Lu C, Fu Y, et al. Progress on Experimental Study of Melt Pool Flow Dynamics in Laser Material Processing. In: Liquid Metals. IntechOpen; 2021. doi: 10.5772/intechopen.97205